Uniformity Level Approach to Fingerprint Ridge Frequency Estimation

Iwasokun Gabriel Babatunde
Department of Computer Science
Federal University of Technology,
Akure, Nigeria

Akinyokun Oluwole Charles
Department of Computer Science
Federal University of Technology,
Akure, Nigeria

Olabode Olatunbosun
Department of Computer Science
Federal University of Technology,
Akure, Nigeria

ABSTRACT
Stages of fingerprint image enhancement include segmentation, normalization, filtering, binarization and filtering. Each of these stages has proved to be very essential for achieving a well enhanced fingerprint image. The major prerequisites to filtering a fingerprint image are ridge orientation and frequency estimations. While ridge orientation estimation is done to obtain the orientation of the ridges, ridge frequency estimation is done with a view to ascertaining the number of ridges within a unit length. The number is useful for fingerprint image filtering. In this paper, a modified fingerprint ridge frequency estimation algorithm is implemented. The modified algorithm consists of stages for estimating ridge orientation and uniformity levels. Two types of images; namely synthetic and real fingerprints were used to evaluate the performance of the algorithm. The results of the evaluation reveal that the modified algorithm shows greater speed and effectiveness than its original version. Facts also emerged on the basic characteristics of the estimates.

General Terms
Image Processing, Pattern Recognition, Security, Algorithms

Keywords
Fingerprint Enhancement, Ridge Frequency Estimation, Biometrics, Uniformity Level

.

1. INTRODUCTION
Facts have continued to emerged that fingerprint is the most universally accepted biometric for various degrees and levels of human identification [1]. Its usefulness and importance are increasingly been recognized in crime investigation, financial transactions, air travels, access monitoring and control, electoral matters and so on. The very wide acceptance of fingerprint for human identity management precipitated the emergence of a good number of Automated Fingerprint Identification Systems (AFIS). Major activities performed in an AFIS include image enhancement, feature extraction and pattern matching. The main essence of image enhancement is to ensure that the system works with images with clean state of health. In other words, for effective and reliable AFIS, fingerprint images with good quality are very important. However, in most cases, majority of the raw images are significantly noisy thereby causing a defect in the system's performance. Images obtained from the same finger but with different levels of noise are presented in Figure 1. A highly noisy image in which the ridges run together is shown in Figure 1(a) while a noisy image due to minimal and high faint ridge structures are shown in Figure 1(b) and 1(c) respectively. The difference in the forms of these images may be due to several reasons including varying application of ink or pressure during manual or electronic fingerprint enrolment [2].

The major effects of noise on fingerprint images include creating false ridge structures appearing as scars, cross-overs, spurs, holes, triangles and spike points [3]. The forms of these false structures are shown in Figure 2. From inspection, it is revealed that the spur structure generates false ridge endings, while both the hole and triangle structures generate false bifurcations. The spike structure on its own generates a false bifurcation and a false ridge ending point.

(a) First impression (b) Second impression (c) Third impression

Fig. 1: Three different impressions of the same finger with different noise levels

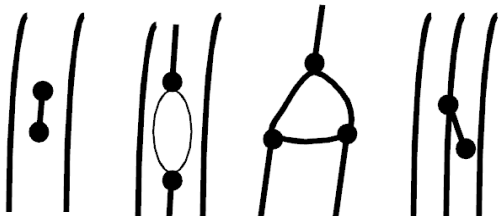

(a)Spur (b)Hole (c)Triangle (d)Spike

Fig. 2: False ridge structures

These false structures result in the extraction of false minutiae points [3] which culminate in system with misleading results due to false acceptance or false rejection. To avoid false results, the fingerprint images are firstly enhanced for the removal of noises and other contaminations. The major stages of the fingerprint image enhancement are conceptualized in Figure 3 [4 - 6]. Each stage is important for obtaining an enhanced fingerprint image in form of a thinned or skeleton image where all forms of overlap in the ridge structure have been eliminated.

As shown in Figure 3, there are two basic prerequisites for fingerprint filtering; namely ridge orientation estimation and ridge frequency estimation. The orientation estimates of each pixel in the image plays contributing role in the estimation of the ridge frequency. The ridge frequency on its own is very useful for noise removal by filtering. Several ridge frequency estimation algorithms have been proposed by different authors

each with attendant strengths and weaknesses. In this paper, a detailed discussion on the modified form of the ridge frequency estimation algorithm proposed in [5] is presented. Section 2 presents discussion on the usefulness as well as current trend of research in fingerprint ridge frequency estimation while Section 3 presents the modified fingerprint ridge frequency estimation algorithm. The experimental results and the conclusion drawn are presented in Sections 4 and 5 respectively.

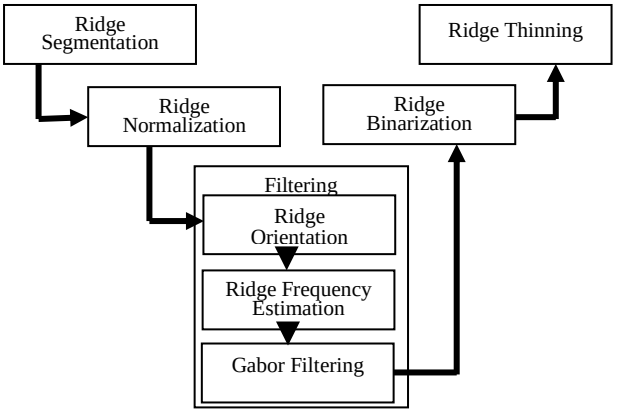

Fig. 3: Stages of fingerprint image enhancement

2. FINGERPRINT RIDGE FREQUENCY

Fingerprint ridge distance is defined as the distance from a given ridge to its adjacent ridges. It is an inter-distance measure from the center of one ridge to the center of the next ridge in both directions. Figure 4 shows enlarged ridge structures with their respective ridge distances.

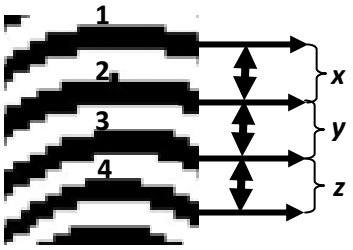

Fig.4: Fingerprint ridges structures and distances

A ridge distance of *x* exists between ridges labeled 1 and 2 while a ridge distance of *y* exists for ridges 2 and 3. Similarly, *z* represents the ridge distance between ridges 3 and 4. Although fingerprint ridge distance is very important in AFIS, it is difficult to estimate due to the following factors [7].

a. Fingerprint images acquired from the same finger but with equipment with different image resolutions may have different ridge distance(s);
b. Even with the same image resolution, noises in form of low contrast, ridge breaks, ridge conglutination and so on, may distort estimations;
c. Occurrence of minutiae may disturb the estimation of the ridge distance;
d. The existence of high curvature in regions containing singularities makes it difficult to estimate ridge distance in these regions with common methods;
e. Different fingers may have different ridge distances;
f. Within the same fingerprint image, different regions may have different ridge distances.

It has been noted that the issues under (c), (d), and (e) are basic and natural properties of fingerprints while the issues under (a), (b), and (f) are controllable and adjustable for improvement. Ridge frequency is the reciprocal of ridge distance indicating the number of ridges within a unit length of an image. It is the local frequency of the ridges that collectively form the ridge frequency image.

The estimation of ridge frequency is one basic prerequisite in the enhancement of fingerprint images. The authors in [8, 9] proposed fast enhancement algorithms which can adaptively and effectively improve the clarity of ridge and valley structures of fingerprint images. The algorithms are based on the estimated local ridge orientations and frequencies. The grey levels along fingerprint ridges and valleys were modeled in [9] as sinusoidal shaped wave along the direction normal to the local ridge orientation. The wave is majorly utilized for the estimation of the ridge frequency based on the assumptions that valid ridge frequencies lie between 1/31 and 1/25 for 500dpi images [8]. The authors in [10] present some improvements to the method in [8] by using a unique anisotropic filter adapted to fingerprint images. In [11], the ridge frequency is obtained by employing the directional projection with the acquired ridge direction. Since the direction of the ridge is previously known, the ridge image is projected onto the perpendicular axis of the given ridge direction. The projection data provide the frequency of the ridge lines in the current block. The authors in [12] present a multi-step algorithm for obtaining the frequency of fingerprint ridges. At each step, an estimated value of the ridge frequency is obtained thereby allowing for any discrepancy with the actual ridge frequency estimate generated due to measurement error as well as the presence of minutiae. A resolution based approach to fingerprint ridge frequency estimation devoid of the specificity of enrolment tools (scanners) is proposed in [13]. The method allows very precise calculation of fingerprint ridge frequency and reference point. In [14] a method of fingerprint pre-classification based on the ridge frequency replacement by the density of edge points of the ridge boundary is proposed. The prerequisites to applying this method are fingerprint image filtering, binarization and marking of good or bad image areas. The method does not require preliminary fingerprint sub-division into sub-blocks but gives room for direct evaluation of the ridge frequency in the areas containing minutiae, singular points or curved capillary lines. A platform comprising of traditional spectral analysis and statistical methods were used for the estimation of fingerprint ridge frequencies in [7]. The spectral analysis method transforms the representation of fingerprint images from the spatial field to the frequency field and completes the ridge distance estimation in the frequency field. On the other hand, in the statistical method, the ridge directions at block level are firstly calculated. Secondly, a locally adaptive method [15] is used to binarize a fingerprint image at block level so that a value of 1 is assigned to pixels on ridges and 0 is assigned to pixels on furrows. Thirdly, the statistical window and baseline are defined. Next is the determination of the ridge distance distribution in each block image using statistical means before the detection of positions and intervals of all peaks. Finally, the ridge distance and confidence level are estimated. It was reported that for good-quality fingerprint images, there is no dramatic difference in performance between the spectral analysis method and the statistical method. However, when fair or poor quality fingerprint images are used, the performance of the statistical method is superior to that of the spectral analysis method with better average performance on the used images. The reported disadvantage of the statistical method is that it performs poorly in regions where there is acute variation of ridge directions.

3. THE PROPOSED ALGORITHM

The proposed ridge frequency estimation algorithm is an extension of the algorithm proposed in [5]. The major activities of the algorithm are the computation of the local orientations and the consistency level of the orientation field. The estimation of local orientation involves the following:

a. Partition the image into blocks of uniform size Q x Q.
b. Compute $\partial_x(p,q)$ and ∂_y(p,q) for each block centered at pixel (p,q) as the gradient magnitudes in the *x* and *y* directions, respectively. ∂_x(p,q) was computed using the horizontal Sobel operator while ∂_y(p,q) was computed using the vertical Sobel operator [4].
c. Estimate the local orientation of the center pixel (r,s) for each block by using the formula:

$$V_x(r,s) = \sum_{p=a}^{b}\sum_{q=c}^{d} 2\partial_x(p,q)\partial_y(p,q) \quad (1)$$

$$V_y(r,s) = \sum_{p=a}^{b}\sum_{q=c}^{d} \partial_x^2(p,q) - \partial_y^2(p,q) \quad (2)$$

$$\theta(r,s) = \frac{1}{2}\tan^{-1}\frac{V_y(r,s)}{V_x(r,s)} \quad (3)$$

$a = r - 0.5Q$, $b = r + 0.5Q$, $c = s - 0.5Q$, $d = s + 0.5Q$ and $\theta(r,s)$ is the least square estimate of the local orientation of the block centered at pixel (r,s).

The uniformity level of the orientation field in the local neighborhood of a pixel (c,d) is then computed by using the following formula:

$$U_o(c,d) = m^{-2}\left(\sum_{(r,s)\in N} |\theta(r,s) - \theta(c,d)|^2\right)^{0.5} \quad (4)$$

$$|\theta(r,s) - \theta(c,d)|^2 = \begin{cases} v & if\ 180 > v \\ v - 180 & otherwise \end{cases} \quad (5)$$

$$v = (\theta(r,s) - \theta(c,d) + 360) mod\ 360 \quad (6)$$

N represents the local neighborhood around (p,q), which is an m x m local window, θ(r,s) and θ(c,d) are local ridge orientations at pixels (r,s) and (c,d) respectively.

If the uniformity level falls below a certain threshold F_c, the local orientations for this region are re-computed by using lower image resolution level. This is repeated until the uniformity is above F_c. The image is then subjected to the following adaptive filters:

$$h_t(c,d,e,f) = \begin{cases} (e^{\delta^{-2}})(2\pi\delta)^{-0.5}, & if \quad e = l(f) - w, \quad f \in \rho \\ -(e^{\delta^{-2}})(2\pi\delta)^{-0.5}, & if \quad e = l(f), \quad f \in \rho \\ 0, & otherwise \end{cases} \quad (7)$$

$$h_b(c,d,e,f) = \begin{cases} (e^{\delta^{-2}})(2\pi\delta)^{-0.5}, & if\ e = l(f) + w, \quad f \in \rho \\ -(e^{\delta^{-2}})(2\pi\delta)^{-0.5}, & if \quad e = l(f), \quad f \in \rho \\ 0, & otherwise \end{cases} \quad (8)$$

$$l(f) = ftan(\theta(c,d)); \quad (9)$$

$$w = Y(2\cos(\theta(c,d))^{-1}, \quad (10)$$

$$\rho = Y[|(-2)^{-1}(\sin(\theta(c,d))|, |(2)^{-1}(\sin(\theta(c,d))|] \quad (11)$$

The two filters are used to stress under different conditions, the local maximum grey level values along the normal direction of the local ridge orientation. The normalized image is convolved with these two masks. If both the grey level values at pixel (c,d) of the convolved images are larger than a certain threshold F_{ridge}, then pixel (c,d) is labeled as a ridge.

4. EXPERIMENTAL RESULTS

The implementation of the proposed algorithm was carried out in an environment characterized by Windows Vista Home Basic Operating System on a Pentium IV 2.10 GHZ of RAM with MATLAB as frontend engine. Towards a succinct performance analysis, both synthetic and real fingerprint images of various qualities were used for the experiments. The synthetic images were obtained using the *circsine* function [16]. Different levels of artificial noise were introduced into the synthetic images using the MATLAB *imnoise* function. Standard fingerprint images contained in FVC2004 fingerprint database with four different datasets obtained from different sources were used. Variation in the datasets sources is useful for monitoring the performance of the algorithm with images from different sources.

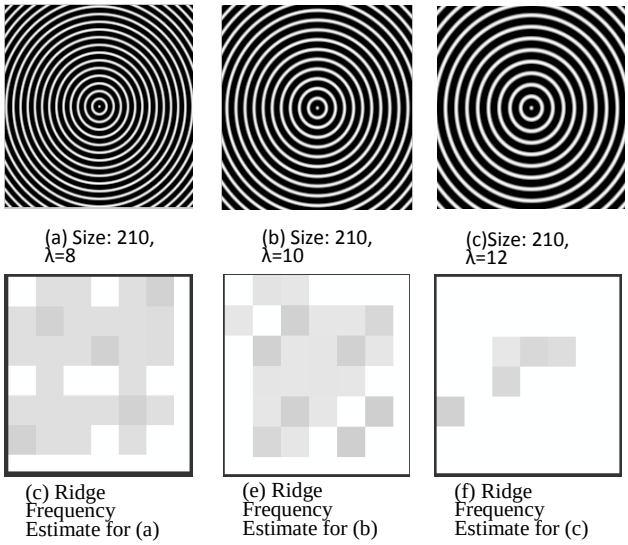

Figure 5: Synthetic images and their ridge

Synthetic images of uniform size 210 by 210 but with wavelengths of 8, 10 and 12 are shown in Figure 5(a), 5(b) and 5(c) respectively. The results of ridge frequency estimation experiments on each of these images are shown in Figures 5(d), 5(e) and 5(f) respectively. The patterns of the ridge frequency estimates for the 32 x 32 size blocks are observed to show variations. This signifies multiple intensity levels across these regions or blocks. The higher the estimate for each of the blocks, the higher is the grey level intensity. Peak value estimates are represented with significantly dark blocks while zero value estimates are represented by white blocks.

Significant variations in the number of blocks with peak, medium and zero value estimates in Figure 5(d), 5(e) and 5(f) revealed that pixels wavelength plays important role in the final estimate. The basic law of increasing wavelength tends

to reducing frequency is obeyed. In this case, the frequency estimates assumed reducing trend with increase in wavelength as the estimates for most blocks evaluate to zero for increasing wavelength. This is revealed by larger number of white blocks for Figure 5(f).

Figure 6 presents a graphical representation of the average non-zero ridge frequency estimates (ANZ) for noise-free synthetic images of size 210, 310 and 410 and wavelengths ranging from 6 to 15. ANZ is the mean ridge frequency estimate for all blocks with non-zero estimates. It is revealed from the plots that ANZ assumed close values for the three images under low wavelengths (6-8) with a range of less than 0.01. In the wavelength range of 9-11, the differences in ANZ become more noticeable with the range increasing to about 0.02. For wavelengths above 11, the differences in the ANZ assumed very wide difference. These results indicate that the ridge estimates tend to same values irrespective of image size for low wavelengths. With higher wavelengths, significant differences emerge for images of different sizes. The results also show that the ANZ values assume no definite pattern with varying wavelengths and image sizes as demonstrated by plots of Figure 6 with numerous turning points.

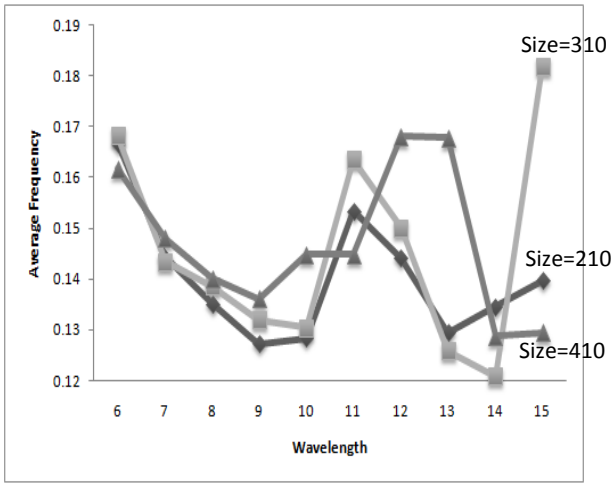

Fig. 6: Graphical representation of the ANZ for synthetic images of different sizes

The ANZ plots for synthetic images with different conditions of noise are presented in Figure 7. These plots were obtained with a view to demonstrate the performance of the algorithm with increasing salt and pepper noise level. The plots revealed significant changes in pattern compared to what obtained in Figure 6 for noise free synthetic image of size 210. This difference indicates that the performance of the algorithm is affected by noise.

At most wavelengths, the ANZ value is highest for noise level of 0.75 and lowest for 0.25. This indicates increasing, ANZ with increase in noise. It is also noticed that the peak values of ANZ are obtained at lowest wavelengths while the values at the higher wavelengths show no potential to rise above the peak. These values indicate that though there is shift in the actual ridge frequency estimates due to noise, the obtained values decrease with increase wavelength. The shape of the plots reveals that the ANZ values are confined to a specific range for the three noise levels.

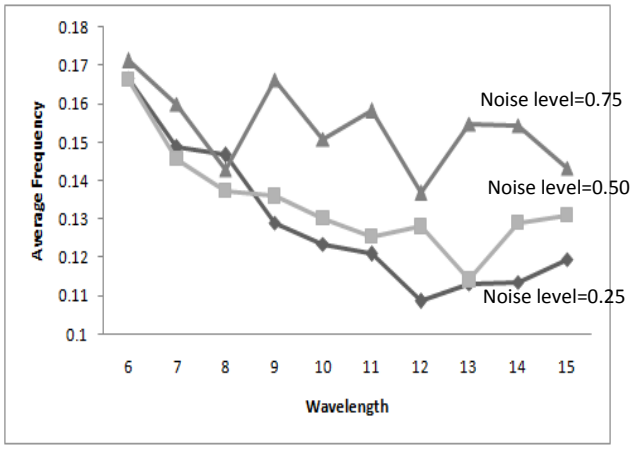

Fig. 7: ANZ plots for synthetic image of size 210 at different noise levels

Figures 8 and 9 present the plots for different noise levels synthetic images of size 310 and 410 respectively. It is observed that at noise level 0.25 and 0.50, just like in Figure 7, there is a near-collapse of the ANZ values at all wavelengths for the two images.

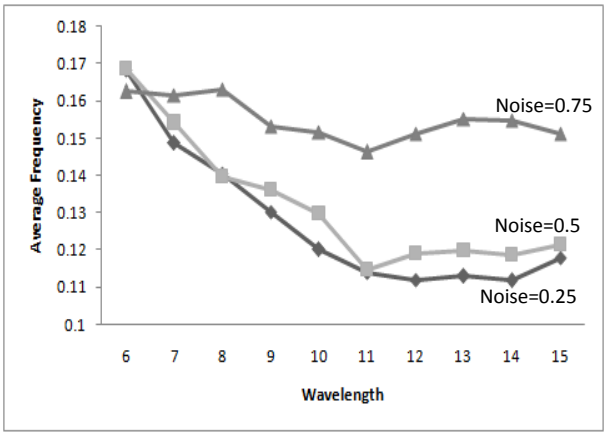

Fig. 8: ANZ plots for synthetic image of size 310 at different noise levels

This closeness indicates that for these noise levels and image sizes, ANZ values are not principally affected. For noise level of 0.75, it is observed that as in the case in Figure 7, the ANZ values are far apart to the values obtained for the lower noise levels for nearly all the wavelengths. This suggests that there is substantial increase in the ANZ values at this noise level. The closeness in the pattern of the plots in Figures 8 and 9 indicates that size plays minimal role in ridge frequency estimation.

The efficiency of the ridge frequency estimation algorithm was quantitatively measured by estimating the Mean Square Error (MSE) which is the difference between the estimated and actual ridge frequency values in radians. The MSE results

for the synthetic image of size 210, 310 and 410 under different conditions of noise are shown in Table 1, 2 and 3 respectively.

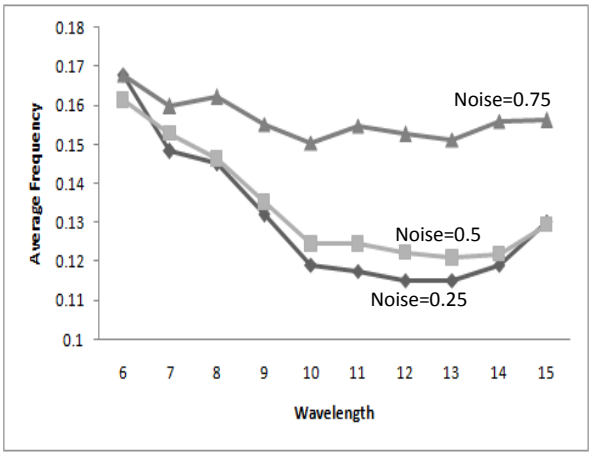

Fig. 9: ANZ plots for synthetic image of size 410 at different noise levels

Table 1: MSE for synthetic image of size 210

S/No.	Noise Level	MSE
1	0.1	0.0000156
2	0.2	0.0000180
3	0.3	0.0000825
4	0.4	0.0004774
5	0.5	0.0006978
6	0.6	0.0014942
7	0.7	0.0044675
8	0.8	0.0071508
9	0.9	0.0078461
10	1.0	0.0084378

The increasing mean square errors in all cases reveal that the accuracy of the algorithm decreases with increase in the noise level irrespective of size. The MSE values recorded in Tables 1, 2 and 3 produces standard deviation of 0.00354, 0.00404 and 0.00400 respectively. These present the degree of spread of the MSE values over the noise range.

Table 2: MSE for synthetic image of size 310

S/No.	Noise Level	MSE
1	0.1	0.0000174
2	0.2	0.0000194
3	0.3	0.0000315
4	0.4	0.0000940
5	0.5	0.0006248
6	0.6	0.0017104
7	0.7	0.0045584
8	0.8	0.0073650
9	0.9	0.0083729
10	1.0	0.0104828

The closeness of the standard deviation figures for the three images also established the claim that size plays insignificant role in ridge frequency estimation. The plots of the MSE values presented in Table 1, 2 and 3 are shown in Figure 10. The collapsing trend of the three plots established the closeness of the standard deviation and a boost to the claim that size plays insignificant role in ridge frequency estimation.

Table 3: MSE for synthetic image of size 410

S/No.	Noise Level	MSE
1	0.1	0.0000147
2	0.2	0.0000302
3	0.3	0.0000511
4	0.4	0.0002909
5	0.5	0.0007166
6	0.6	0.0014711
7	0.7	0.0030360
8	0.8	0.0076624
9	0.9	0.0088897
10	1.0	0.0098269

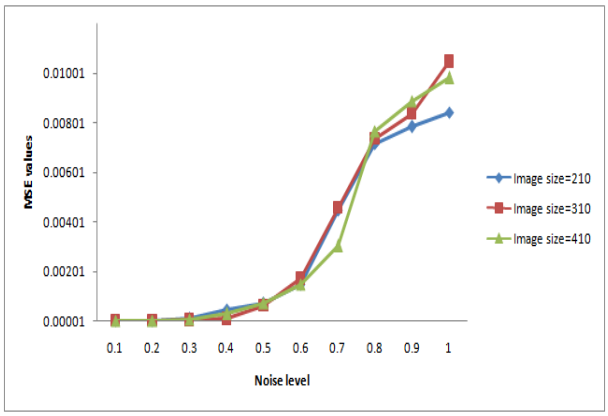

Fig. 10: Plots of MSE values for images of different size and noise levels

Experiments were also based on the tests from a standard Fingerprint Verification Competition (FVC). The experiments measured ANZ values for FVC2004 datasets DB1, DB2, DB3 and DB4. The four datasets were of different qualities with each containing 80 fingerprints. The 80 fingerprints are made up of 16 fingerprints from 5 different persons. Dataset DB1 and DB2 were acquired using an optical fingerprint reader, dataset DB3 was acquired using a capacitive fingerprint reader, and dataset DB4 was obtained with computer assistance, using the software SFinGE.

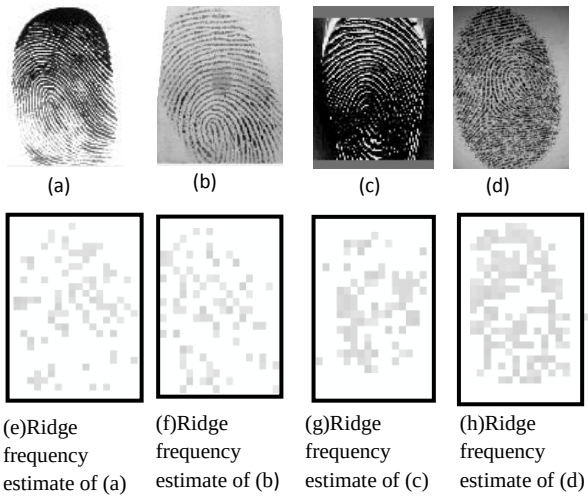

Fig. 11: Selected images and their ridge frequency estimates

Figure 11 (a-d) presents some selected images in the four datasets. The images of ridge frequency estimates for Figure 11(a), 11(b), 11(c) and 11(d) are shown in Figure 11(e), 11(f), 11(g) and 11(h) respectively. These images show significant differences due to unequal fingerprints contrasts and wavelengths. In view of this, synthetic images which possess controllable or adjustable contrast and wavelengths are more suitable for evaluating the performance of the algorithm.

The results of the ANZ experiments on the four datasets presented in Table 4 show that the ANZ values for the datasets fall within same range. This indicates closeness in the non-zero estimates for the four datasets even though they were obtained from different sources.

Table 4:ANZ values for Datasets contained in FVC2004 fingerprint database

S/No.	Dataset	ANZ	Standard Deviation
1	A	0.1301	0.0083
2	B	0.1115	0.0089
3	C	0.1224	0.0101
4	D	0.1364	0.0124

The results of an experiment conducted for measuring the completion time in seconds for the original version proposed in [5] and the modified version on the four datasets contained in FVC2004 fingerprint database is presented in Table 5. It is revealed from the Table that for all datasets, the modified algorithm completes at shorter times. The highly significant difference in the completion time is attributed to the block processing approach in which the orientation of the center pixel is only computed. The other pixels in every block then assume the orientation estimate for its center pixel. This leads to fewer computations and subsequently lesser completion time when compared to the original algorithm in which the orientation estimate is computed for all the pixels.

Table 5:Completion for original and modified algorithm on four datasets

S/No.	Dataset	Original	Modified	% Increase
1	A	1.563	0.750	52.02
2	B	1.317	0.600	54.44
3	C	1.015	0.450	55.67
4	D	1.264	0.587	53.56

5. CONCLUSION

Fingerprint ridge frequency estimation, which is a fundamental component of fingerprint enhancement, has been discussed in this paper. The implementation of a modified version of a ridge frequency estimation algorithm proposed in [5] was carried out. The modified algorithm has stages for ridge orientation estimation and its uniformity level. The new approach used block processing approach in place of the pixel processing approach of the original algorithm. Indicators emerged that the new algorithm does well when compared with its original version. Obtained results showed the dependence of the algorithm on the quality of the image. Results also show that the ridge frequency and the average non-zero ridge frequency estimates (ANZ) diminish with increase image wavelengths. Analysis of the obtained results equally showed that size of image plays no significant role in ridge frequency estimation.

The results of measurement of completion time for the original and modified algorithms on the four datasets of standard FVC2004 fingerprint database show that the modified algorithm has well over 50% better completion time for all the datasets. The reduced completion time is attributed to the considerable reduction in the number of calculation in the modified algorithm.

6. REFERENCES

[1] Roberts C. 2005. Biometrics' (http://www. ccip. govt.nz/newsroom/information_notes/2005/biometrics.pdf). Accessed 12/07/2006

[2] Anil K. J., Jianjiang F and Karthik N. 2010. Fingerprint Matching, IEEE Computer Society, page 36-44

[3] Iwasokun G. B., Akinyokun O. C., Alese B. K. & Olabode O. 2011. Adaptive and Faster Approach to Fingerprint Minutiae Extraction and Validation. International Journal of Computer Science and Security, Malaysia, Volume 5 Issue 4, page 414-424.

[4] Iwasokun G. B., Akinyokun O. C., Alese B. K. & Olabode O. 2012. Fingerprint Image Enhancement: Segmentation to Thinning, International Journal of Advanced Computer Science and Applications (IJACSA), Indian, Vol. 3, No. 1, 2012

[5] Hong L., Wau Y. and Anil J. 2006. Fingerprint image enhancement: Algorithm and performance evaluation, Pattern Recognition and Image Processing Laboratory, Department of Computer Science, Michigan State University, pp1-30

[6] Raymond T. 2003. Fingerprint Image Enhancement and Minutiae Extraction, PhD Thesis Submitted to School of Computer Science and Software Engineering, University of Western Australia, pp21-56.

[7] Yilong Y., Jie T. and Xiukun Y. 2002. Ridge Distance Estimation in Fingerprint Images: Algorithm and Performance Evaluation, EURASIP Journal on Applied Signal Processing Vol. 4, 495–502

[8] Hong, L., Wan, Y. & Jain, A. 1998. Fingerprint Image Enhancement: Algorithm and Performance Evaluation. IEEE Transactions on Pattern Analysis and Machine Intelligence 20: 777–789

[9] Arun Vinodh C. 2007. Extracting and Enhancing the Core Area in Fingerprint Images, IJCSNS International Journal of Computer Science and Network Security, VOL.7 No.11, pp16-20

[10] Greenberg S. Aladjem M. and Kogan D. 2002. Fingerprint Image Enhancement Using Filtering Techniques, Elsevier Science Ltd, pg 227-236

[11] Byung-Gyu K., Han-Ju K. and Dong-Jo P. 2002. New Enhancement Algorithm for Fingerprint Images, IEEE, 1051-4651/02 $17.00

[12] Devansh A. and Anoop N. 2011. Fingerprint Feature Extraction from Gray Scale Images by Ridge Tracing, IEEE, 978-1-4577-1359-0/11/$26.00

[13] Porwick P. and Wieclaw L. 2009: A new fingerprint ridge frequency determination method, IEICE Electronics Express, Vol. 6, No. 3 pages 154-160

[14] Malickas A. and Rvitkus R. 2000. Fingerprint Pre-Classification Using Ridge Density, INFORMATICA, Institute of Mathematics and Informatics, Vilnius, Vol. 11, No. 3, 257–268 257

[15] Bernsen J. 1986. Dynamic thresholding of grey-level images, in Proceedings of the 8th International Conference on Pattern Recognition, Paris, France, pp.1251–1255.

[16] Kovesi, P. 2002. MATLAB functions for computer vision and image analysis. School of Computer Science and Software Engineering, The University of Western Australia.http://www.cs.uwa.edu.au/pk/Research/Matlab Fns/index.html. Accessed: 21 March 2009